NASA TECHNICAL MEMORANDUM
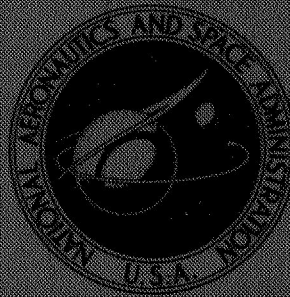
EFFECT OF VARIABLE STATOR AREA ON PERFORMANCE OF A SINGLE-STAGE TURBINE SUITABLE FOR AIR COOLING

I. Stator Overall Performance With 130-Percent Design Area

by Edward M. Szanca, Frank P. Behning, and Harold J. Schum

Lewis Research Center
Cleveland, Ohio

EFFECT OF VARIABLE STATOR AREA ON PERFORMANCE OF

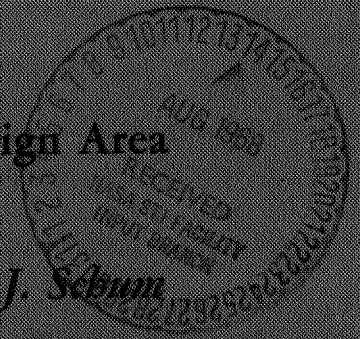# A SINGLE-STAGE TURBINE SUITABLE FOR AIR COOLING

I. Stator Overall Performance With 130-Percent Design Area

By Edward M. Szanca, Frank P. Behning, and Harold J. Schum

Lewis Research Center
Cleveland, Ohio

NATIONAL AERONAUTICS AND SPACE ADMINISTRATION

ABSTRACT

The turbine is being investigated at stator area settings of 70, 100, and 130 percent of design. This report presents the overall stator performance at the open setting and compares the results with those obtained from design tests. Results are presented in terms of weight flow, outlet flow angle, blade surface static pressure and velocity distributions, as well as inner and outer wall static pressures as obtained over a stator pressure ratio range.

EFFECT OF VARIABLE STATOR AREA ON PERFORMANCE OF

A SINGLE-STAGE TURBINE SUITABLE FOR AIR COOLING

I. Stator Overall Performance With 130-Percent Design Area

by Edward M. Szanca, Frank P. Behning, and Harold J. Schum

Lewis Research Center

SUMMARY

As part of a program directed at the study of variable stator turbines, a single-stage unit is being investigated with the stator in positions opened and closed from that of design. This report presents the results of the experimental investigation of the overall performance of the stator component in the opened position. This position was set so that the channel exit orthogonal at the mean section was 130 percent that of the design value. The stator performance characteristics presented include that of weight flow, outlet flow angle, blade surface static pressure and velocity distributions, as well as inner and outer wall static pressures as obtained over a stator pressure ratio range.

The results of the investigation indicated that the stator operated as a convergent-divergent blade row at this setting with this effect being most pronounced at the tip section. The mass flow was found to be greater than that corresponding to the area change at subsonic flow conditions and less than that at choked conditions. The measured blade exit flow angle and radial static pressure distribution were close to that expected over the operating range covered. The small deviation in angle observed in the hub region could be the result of radial equilibrium effects and channel blade exit flow area variations.

The blade surface static pressure measurements also indicated the shift of the throat upstream of the channel exit, particularly at the tip region. This shift was due to the channel area redistribution and the resulting large velocity peaks which existed on the suction surface in this region. The static pressure measurements at the hub and tip channel exits also appeared to reflect the convergent-divergent nature of the tip section. At the hub, a single curve typical of a convergent section was obtained. At the tip, the curve appeared to branch into two parts at higher pressure ratios.

INTRODUCTION

Advanced aircraft, such as the supersonic transport, require high performance engines to accomplish their mission goals. The trend in the design of these engines is towards the use of higher turbine inlet temperatures by employing turbine cooling. In addition, such designs must include considerations of maintaining high performance at each of the widely varying modes of operation encountered over the aircraft operating range. One method considered (refs. 1 and 2) is the use of variable turbine geometry as a means of permitting the engine to operate at optimum cycle conditions as flight conditions vary. Such turbines would typically have adjustable stators to vary the flow rate for a given turbine pressure ratio, thereby representing off-design conditions of operation for the turbine. It is of course desirable to maintain high turbine efficiency at these off-design conditions of operation.

In order to better understand the performance characteristics of turbines incorporating variable stator area, one such turbine has been under investigation at the Lewis Research Center. This is a 30-inch (0.762-m) tip diameter scale-model turbine, typical of the first stage of a turbine for a supersonic turbojet engine. The blading was designed with allowance for both stator and rotor cooling. The design and overall stator performance of this turbine at the design stator setting is described in reference 3. The stator boundary layer characteristics are presented in reference 4, and stage performance data are presented in reference 5. This was considered to be the reference-design, or 100-percent stator area, turbine for the variable geometry studies.

Two additional stator assemblies were fabricated in order to provide a range of flow rates. The stator assemblies had flow areas determined at the exit channel orthogonal of the mean blade section of 70 and 130 percent of design. Both cold air stator tests and stage performance tests were conducted for each stator assembly. This report presents the results of the first phase of these tests, namely, the overall stator performance of the 130-percent flow area stator. This stator will be designated as the subject opened stator and that stator with design setting as the reference design stator. The variation in mass flow rate, blade surface velocity distribution, and exit flow angle are presented over a range of stator pressure ratios. The results are compared to those obtained from the test of the reference design stator.

SYMBOLS

p   absolute pressure, lb/ft^2; N/m^2

r   radius, in.; m

V   absolute gas velocity, ft/sec; m/sec

2

w	mass flow rate, lb/sec; kg/sec
α	absolute gas flow angle measured from axial direction, deg
δ	ratio of inlet pressure to U.S. standard sea-level pressure
θ_{cr}	squared ratio of critical velocity at turbine inlet to critical velocity of U.S. standard sea-level air
φ	blade orientation angle measured from axial direction, deg

Subscripts:

cr	condition at Mach 1
d	station downstream of turbine stator
h	hub (inner wall)
i	station at stator blade exit orthogonal
t	tip (outer wall)
0	station at turbine inlet
1	station at stator outlet free stream

Superscript:

'	total state condition

STATOR MODIFICATION

As indicated in the INTRODUCTION, the setting of the subject opened stator was determined by increasing the mean section channel exit orthogonal length to a value 30 percent greater than that of the design reference stator. Figure 1 presents the blade positions at the mean section for both stators and indicates that the blade profiles were oriented about the center of the trailing edge. This was done to maintain radial trailing edges for stator exit surveys. In conjunction with the change in flow area, the associated orientation angle φ was decreased from 41.03° to 32.59°, a change of 8.44°. This change in angle setting was of course constant radially and resulted in an increase at the hub and tip station exit orthogonals of 35 and 26 percent, respectively.

A complete description of the procedure used in arriving at the blade profile, and a tabulation of the blade coordinates, can be found in reference 3. From observation of the mean profile (fig. 1), it is evident that blading of the type suitable for air cooling was used.

The stator assembly was actually built as a separate unit with the blading oriented in

the opened position for the test program. This was done for simplicity and to avoid the complex mechanisms involved in making the stator fully variable.

APPARATUS, INSTRUMENTATION, AND PROCEDURE

The test facility used in this program was designed to incorporate a complete research turbine. A photograph of the test facility is shown in figure 2. This phase of the investigation, however, was concerned with evaluating the overall performance of the opened stator configuration, when tested as a separate component. A photograph of the reference design stator installed in the facility (which is similar to the subject opened stator) is shown in figure 3.

Apparatus

The apparatus consisted of the subject opened stator assembly and test sections, together with suitable ducting and control valves. A diagrammatic sketch of the turbine stator test section is shown in figure 4. The stator had a 30-inch (0.762-m) outside diameter. It is comprised of a full annular cascade of 50 hollow, cast, stainless-steel blades. The blade height was 4 inches (0.1016 m). As mentioned in the STATOR MODIFICATION section, the blades were oriented so as to provide a mean section channel exit orthogonal length 30 percent greater than the reference design stator.

Dry pressurized air was supplied to the test section from a combustion air system. The air flow was measured with a calibrated Dall tube type venturi meter. Turbine inlet pressure was controlled by butterfly throttle valves located between the venturi meter and the turbine inlet plenum chamber. Air leaving the stator was ducted to the altitude exhaust system. The stator outlet pressure was controlled by butterfly throttle valves located downstream of the test section.

Instrumentation

The subject opened stator test section was instrumented similarly to the reference design turbine stator test section (ref. 3). At each of four measuring stations (fig. 4) were located eight static pressure taps, four each at the inner and outer walls. The inner wall and outer wall taps were located opposite each other. At the stator inlet and the downstream measuring stations, 0 and d, respectively, the pressure taps were spaced about 90° apart around the circumference. Hub and tip static-pressure taps at station i

4

were situated at the center of the exit orthogonal labeled A in figure 5. At station 1, the pressure taps were at the mean streamline of the free stream flow. The pressure taps at station i were positioned in four stator passages spaced about 90° apart to the nearest passage. The pressure taps at station 1 were located at the exit of these same four passages.

Two thermocouple rakes were located at the stator inlet measuring station spaced 180° apart circumferentially. Each rake contained five thermocouples situated at the area center radii of five equal annular areas.

Four Kiel-type total pressure probes were also located at the inlet to the stator. The probes were positioned at the area center radius and were spaced 90° apart circumferentially.

Each station group of four pressure taps, except those at station d, were manifolded and connected to a single manometer tube. The eight outlet static pressures at station d were individually read on manometer tubes.

A total of 92 static pressure taps was installed on the blade suction and pressure surfaces at the hub, mean, and tip sections of three blade passages. The static pressure taps at the hub and tip sections were located 0.1 inch (0.254 cm) from the inner and outer walls to avoid end wall boundary layers. The mean-section pressure taps were located midway between the inner and outer walls. The location of the blade pressure static taps are shown in figure 5 for the three blade sections. The static pressure taps were distributed approximately equal among the three blade sections.

All pressures were read on mercury fluid manometers except for the venturi differential pressure which was read on a tetrabromoethane fluid manometer. All temperatures were read with a direct-reading self-balancing potentiometer.

The mass flow rate was measured with the Dall tube venturi meter as explained in reference 3. The flow angle at the stator exit (station 1) was measured with a self-aligning angle probe. An x-y plotter recorder stator outlet angle as a function of radial position.

Procedure

The test procedure for the subject opened stator was identical to the test procedure for the reference design stator. Stator inlet total pressure was set at a nominal value of 30 inches of mercury absolute (1.0159×10^5 N/m^2). The inlet temperature was about 70° F (294.3 K). The mass flow data were obtained over a range of overall pressure ratio by varying the outlet pressure.

The static pressures along the blade surfaces and the stator exit flow angle data were obtained at pressure ratios corresponding to nominal outlet hub critical-velocity ratios $\left(V/V_{cr}\right)_{d,h}$ of 0.38, 0.5, 0.7, 0.896 (reference design), 1.1, and 1.3.

RESULTS AND DISCUSSION

The results of the subject investigation are divided into four parts. These include (1) mass flow and radial static pressure distribution, (2) stator outlet flow angle variation, (3) blade surface static pressure and velocity distribution as obtained at the hub, mean, and tip sections, and finally (4) hub and tip wall static pressures as obtained at the channel exit orthogonal. Where appropriate, comparison will be made with results obtained from the reference design stator.

Mass Flow

The experimentally obtained equivalent mass flows $w\sqrt{\theta_{cr}}/\delta$ are shown in figure 6 together with that obtained for the reference design stator setting (ref. 3). Two curves are presented for each stator setting with mass flow plotted as a function of both inner and outer wall total to static pressure ratio at station d ($p_0'/p_{d,h}$ and $p_0'/p_{d,t}$). Also shown is the design pressure ratio at the inner wall (1.705) which represents a stator subsonic operating condition.

From the figure it can be seen that, at the design hub pressure ratio, the corresponding tip ratio is 1.38. This is approximately the same as for the design stator setting. Therefore, it is indicated that, at this condition, the radial variations in static pressure at the stator exit are similar. At this pressure ratio, however, the subject opened stator passed 53.0 pounds per second (24.0 kg/sec), which is an increase of 33 percent of design. In addition, a comparison of the mass flow at the design inner wall total to static pressure ratio indicates it to be only 3 percent below the choking value, whereas that for the design setting is 7 percent below. Thus, it is indicated that the flow limiting area within the subject stator is at a pressure ratio much closer to choke than that of the reference stator.

Further inspection of the figure reveals that the maximum equivalent flow passed by the subject stator was 54.5 pounds per second (24.7 kg/sec), which is only 27 percent greater than the maximum value for the reference stator. This indicates that the actual throat area is less than that anticipated. In addition, this maximum flow occurs at an outer wall total to static pressure ratio of approximately 1.6, which is substantially subsonic. Therefore, it is indicated that the stator in its open position is performing as a convergent-divergent blade row with the flow limiting area upstream from the channel exit, and that this flow area restriction is most severe in the tip region. Further discussion of this aspect will be made in subsequent sections.

6

Outlet Flow Angle

The stator outlet flow angles α_1 are shown in figure 7 as a function of radius ratio r/r_t for the five inner wall total to static pressure ratios $p_0'/p_{d,h}$ corresponding to $\left(V/V_{cr}\right)_{d,h}$ values of 0.38, 0.50, 0.70, 0.896, 1.1, and 1.3. The figure shows a repro-duction of the traces as recorded on the x-y plotter. The wavy form of the traces occur due to over correction of the flow angle by the actuator drive. Also included for compar-ative purposes are calculated curves obtained when considering each section on a two-dimensional basis. This angle variation was computed using the technique described in reference 3 but in a reverse fashion, since in this case, the exit orthogonal length is known and the angle desired.

From the figure it can be seen that reasonably close agreement between the calcu-lated and experimental angle variation occurs in the mean and tip section regions. How-ever, in the hub region there is some deviation of flow angle towards axial. These trends are somewhat different from those for the reference stator where an overturning in the hub region at higher critical velocity ratios was observed. These deviations from the calculated curve could occur due to the velocity diagrams set up by the blading not being consistent with radial equilibrium such that some change in angle would occur as the flow adjusts in the downstream region. As pointed out in the stator modification dis-cussion, the increase in stator exit orthogonal length through the blade orientation was not consistent, but increased in percentage more at the hub than at the tip. Thus, it would be anticipated that a higher through flow component of velocity would occur near the inner wall, thereby contributing to these deviations.

Blade Surface Static Pressure and Velocity Distributions

The surface static pressure distributions along the suction and pressure surfaces at the hub, mean, and tip sections of the stator passage are shown in figure 8. These pres-sure distributions were obtained for a range of outlet inner wall critical velocity ratios from 0.38 to 1.3, inclusively. The curves show the ratio of the surface static pressure to the inlet total pressure plotted as a function of nondimensional blade surface length. Values of 0 and 1 correspond to the leading- and trailing-edge stagnation points. These points, together with the channel tap nomenclature, are shown in figure 5.

The expected general decrease in surface static pressure with increased critical ve-locity ratio can be seen from figure 8. In addition, the position of the choking orthogonal can be approximated by a comparison of the pressure distribution curves at the high critical velocity ratios (1.1 and 1.3). The pressure lines would be expected to be coinci-dent upstream and diverging downstream of the choking position. Although small differ-

7

ences due to data inaccuracy exist, a trend can nevertheless be observed from figure 8. The suction surface pressure distribution shows that the choking location is close to the blade exit at the hub, position A in the figure. The choking location then appears to move upstream within the guided channel with increasing radius. At the tip, the channel is choked well upstream of the blade outlet, and is located close to position E in the figure. The extent of this shift can be noted by comparing position E with position A in figure 5. This shift in throat position is due to (1) a relative change in surface geometry due to the rotation of fixed blade surfaces about their trailing edges, and (2) the resulting high velocity gradients and peaks that occurred in the upstream regions. This aspect will be discussed further by considering the blade surface velocity distributions.

The static pressure data taken at an operating point corresponding to $\left(V/V_{cr}\right)_{d,h}$ = 0.896 was converted into surface critical velocity ratios in accordance with the method described in reference 3. Figure 9 presents the resulting velocity distribution for both the subject and reference stator. Also shown is a calculated velocity distribution obtained using the method of reference 6. This was the same method used for the reference 3 stator design.

Inspection of figure 9 indicates that although the general trends are similar for the two stators, the velocity peak on the suction surface at the tip section has become very severe, moving in the supersonic regime. This shift to higher peak velocities was also predicted analytically and attributed to the combination of high suction surface curvature and change in channel convergence. These peaks occur in the region where a previous discussion has indicated the stator throats to lie.

As was observed for the reference design stator, velocity peaks, somewhat accentuated, also occurred in the leading edge region on the pressure surface. The analysis procedure, confined to the guided channel, did not cover this part of the blade. However, it is thought that these increased peaks occurred due to increased negative incidence into the blade row as the blade passage is opened up.

Channel Exit Pressure Ratios

In the APPARATUS, INSTRUMENTATION, AND PROCEDURE section it was indicated that static pressure taps were located in the center of the exit orthogonal at the hub and tip (orthogonal A, figs. 5(a) and (c)). This was done in anticipation of measuring these pressures to study the stator choking conditions assuming that these orthogonals corresponded to the choking position. From the test results presented, however, it is evident that the tip section is operating in a convergent-divergent manner such that orthogonal A at this section is in the diverging part of the channel. As a consequence, it would be expected that more than one level of total to static pressure ratio might occur

8

at this position.

The experimentally obtained pressure ratios at this station (i) are shown in figures 10(a) and (b). The hub pressure ratio $p_0'/p_{i,h}$ in figure 10(a) is seen to behave in a manner expected for a convergent section, increasing linearly with overall pressure ratio at the hub $p_0'/p_{d,h}$ until choking is reached, and remaining constant thereafter.

Figure 10(b) shows the variation in total to static pressure ratio measured at the tip pressure ratio $p_0'/p_{i,t}$ is plotted as a function of overall pressure ratio at the tip $p_0'/p_{d,t}$. Here it is indicated that the curve branches into two parts - one is subsonic and the other is supersonic. These results then give further evidence as to the convergent-divergent nature of this section.

SUMMARY OF RESULTS

As part of a single-stage turbine variable stator area program, an investigation of the overall performance of the stator in an opened configuration was made. In this configuration, the channel exit orthogonal at the mean section was increased to 130 percent that of the reference design setting. The results of the investigation can be summarized as follows:

1. In its opened position, the stator operated as a convergent-divergent blade row with the mass flow at subsonic conditions being greater than the corresponding area change. At choked flow conditions, the mass flow was less than the corresponding area change. The convergent-divergent effect was most pronounced at the tip.

2. The measured blade exit flow angle and radial static pressure distribution were close to that expected over the operating range covered. Some minor deviations in angle occurred, principally in the hub region, which could be attributed to the combination of radial equilibrium effects and the increase in channel flow area not being constant radially.

3. The blade surface static pressure measurements also indicated the shift of the throat inward from the channel exit, particularly at the tip region. This shift was due to the channel area redistribution and to the resultant high velocity peaks which existed on the suction surface in this region.

4. Static pressure measurements at the hub and tip channel exits also appeared to reflect the convergent-divergent nature of the tip section. A single curve typical of a convergent section was obtained at the hub, whereas the curve appeared to branch into two parts at higher pressure ratios at the tip.

Lewis Research Center,
    National Aeronautics and Space Administration,
        Cleveland, Ohio, April 11, 1968,
           126-15-02-15-22.

REFERENCES

1. Dugan, J. F., Jr.; Koenig, R. W.; Whitlow, J. B., Jr.; and McAuliffe, T. B.:
   Power for the Mach 3 SST. Astron. Aeron., vol. 2, no. 9, Sept. 1964, pp. 44-51.

2. Heaton, Thomas R.; Forrette, Robert E.; and Holeski, Donald E.: Investigation of
   a High-Temperature Single-Stage Turbine Suitable for Air Cooling and Turbine Stator
   Adjustment. I - Design of Vortex Turbine and Performance with Stator at Design
   Setting. NACA RM E54C15, 1954.

3. Whitney, Warren J.; Szanca, Edward M.; Moffitt, Thomas P.; and Monroe, Daniel E.:
   Cold-Air Investigation of a Turbine for High-Temperature-Engine Application. I.
   Turbine Design and Overall Stator Performance. NASA TN D-3751, 1967.

4. Prust, Herman W., Jr.; Schum, Harold J.; and Behning, Frank P.: Cold-Air In-
   vestigation of a Turbine for High-Temperature-Engine Application. II. Detailed
   Analytical and Experimental Investigation of Stator Performance. NASA TN D-4418,
   1968.

5. Whitney, Warren J.; Szanca, Edward M.; Bider, Bernard; and Monroe, Daniel E.:
   Cold-Air Investigation of a Turbine for High-Temperature-Engine Application. III -
   Overall Turbine Performance. NASA TN D-4389, 1968.

6. Katsanis, Theodore; and Dellner, Lois T.: A Quasi-Three-Dimensional Method for
   Calculating Blade Surface Velocities for an Axial Flow Turbine Blade. NASA TM
   X-1394, 1967.

10
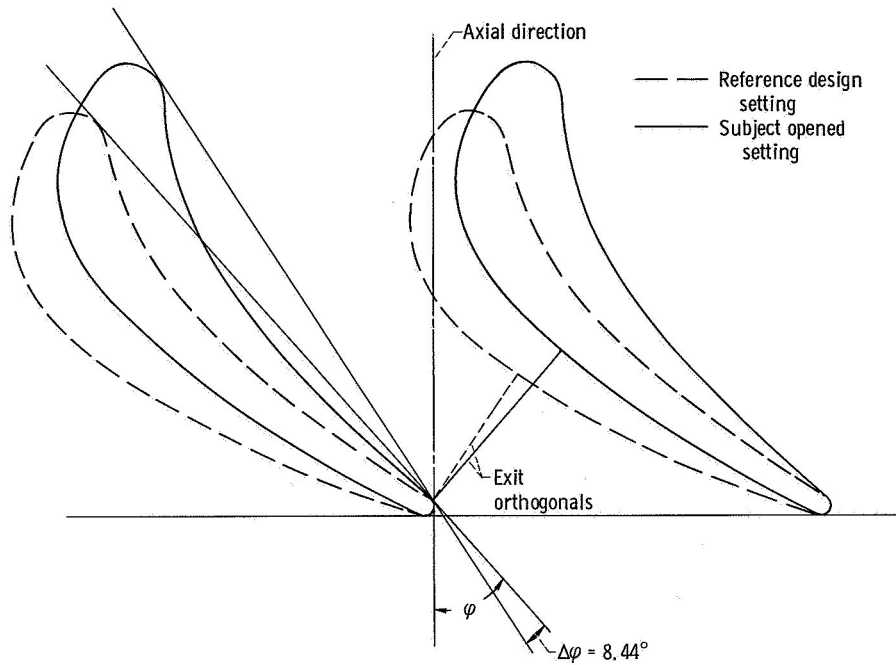
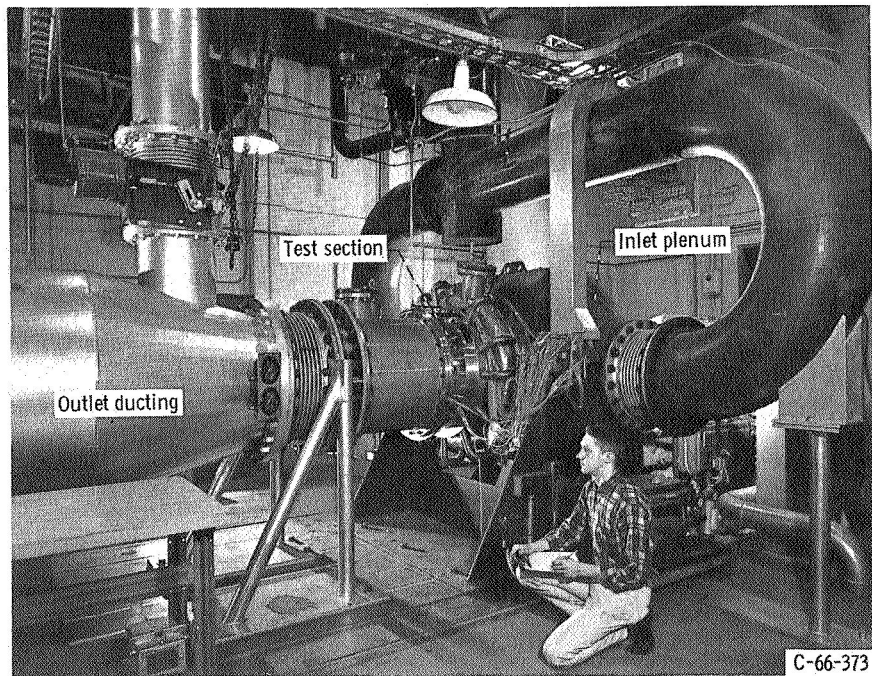Figure 1. - Stator blade orientation at mean section.
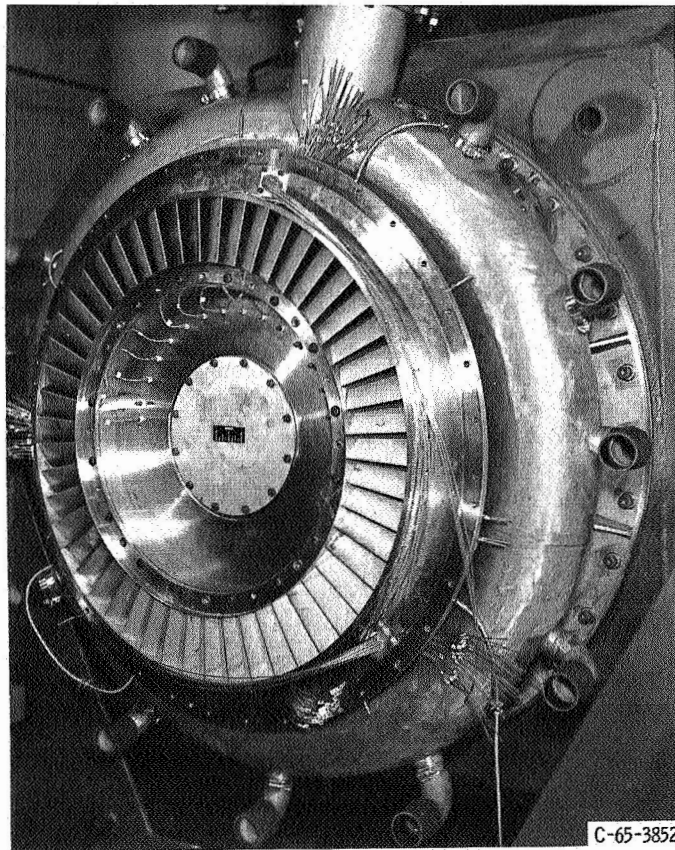

Figure 2. - Test facility.

Figure 3. – Stator assembly installed in test facility.

C-65-3852
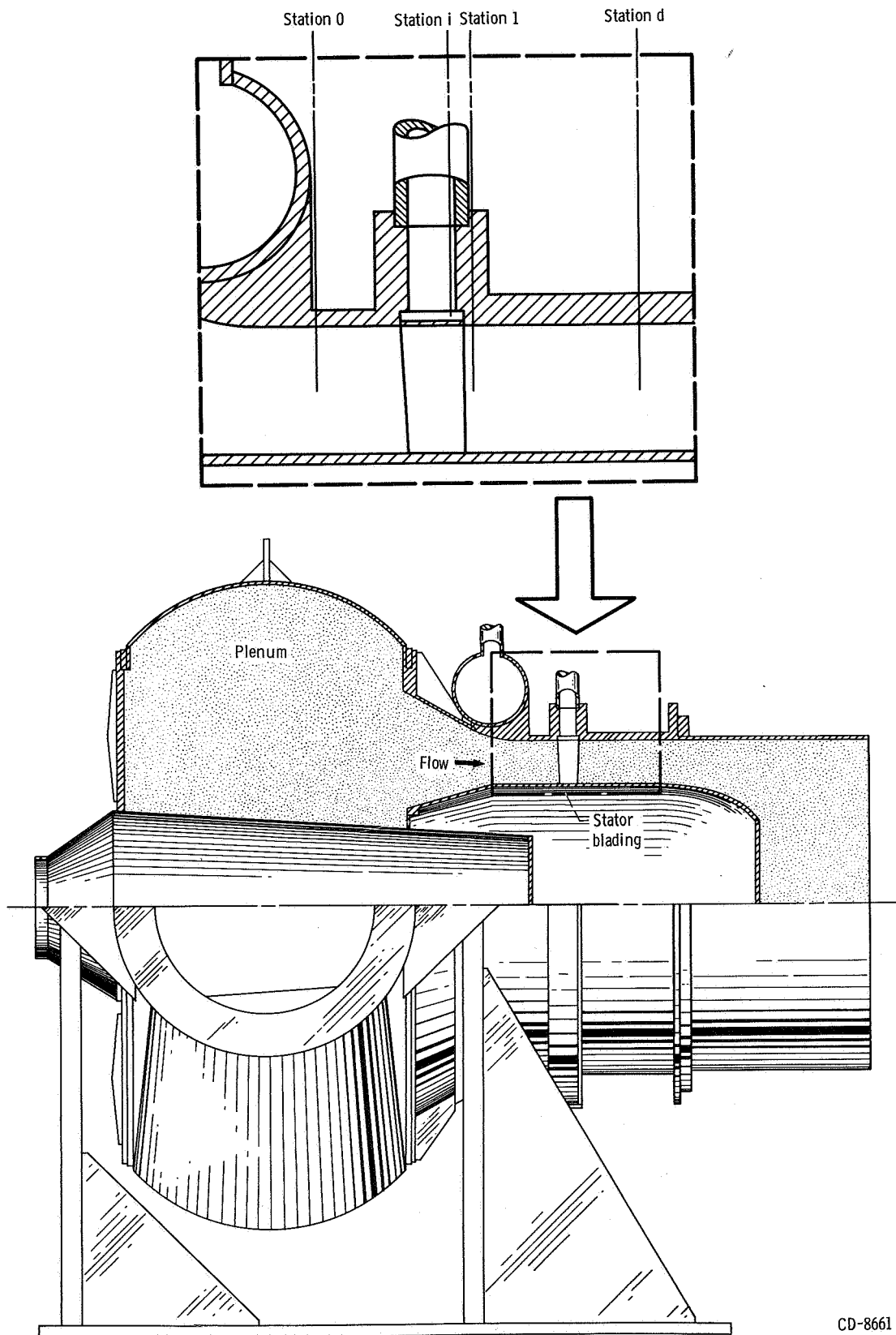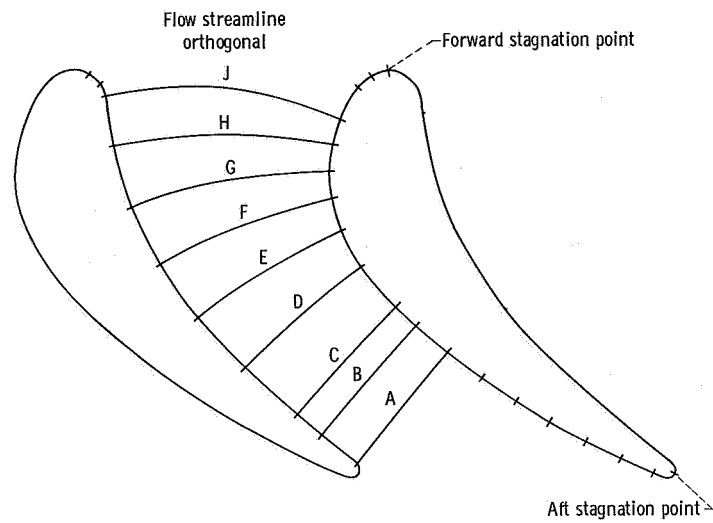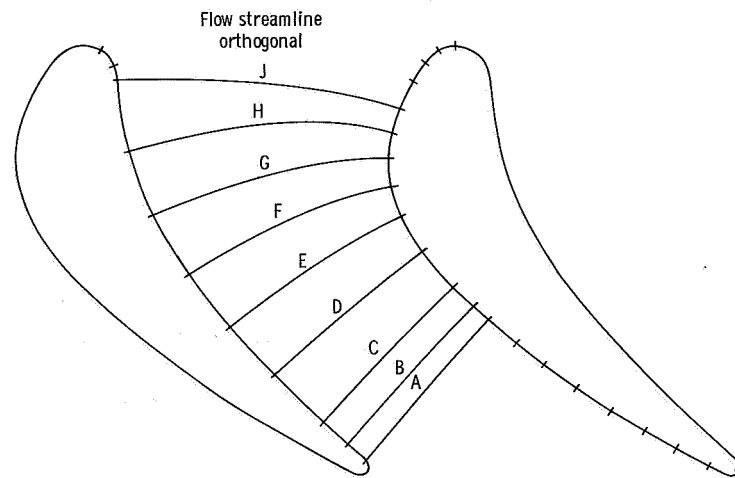
Station 0   Station i Station 1   Station d

Plenum

Flow

Stator
blading

CD-8661

Figure 4. - Schematic diagram of turbine-stator test section.

13

Flow streamline
orthogonal

Forward stagnation point

J

H

G

F

E

D

C

B

A

Aft stagnation point

(a) Hub section, 30 taps.

Flow streamline
orthogonal

J

H

G

F

E

D

C

B

A

(b) Mean section, 32 taps.

Flow streamline
orthogonal

H

G

F

E

D

C

B

A
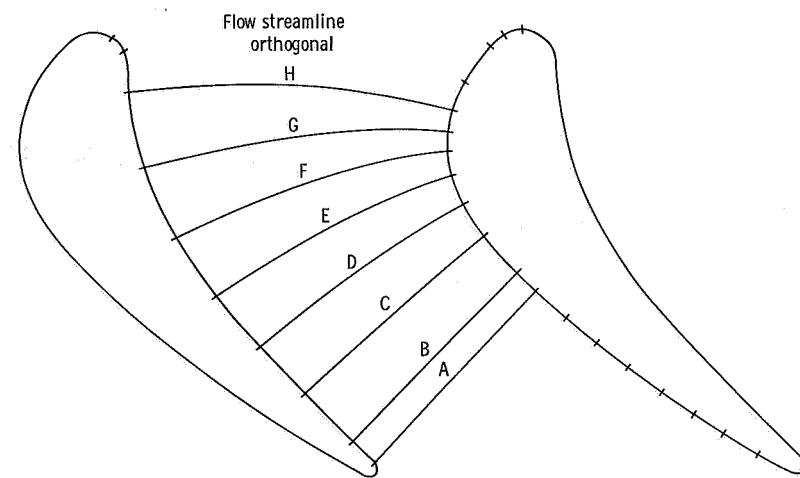
(c) Tip section, 30 taps.

Figure 5. – Static pressure tap location.

14
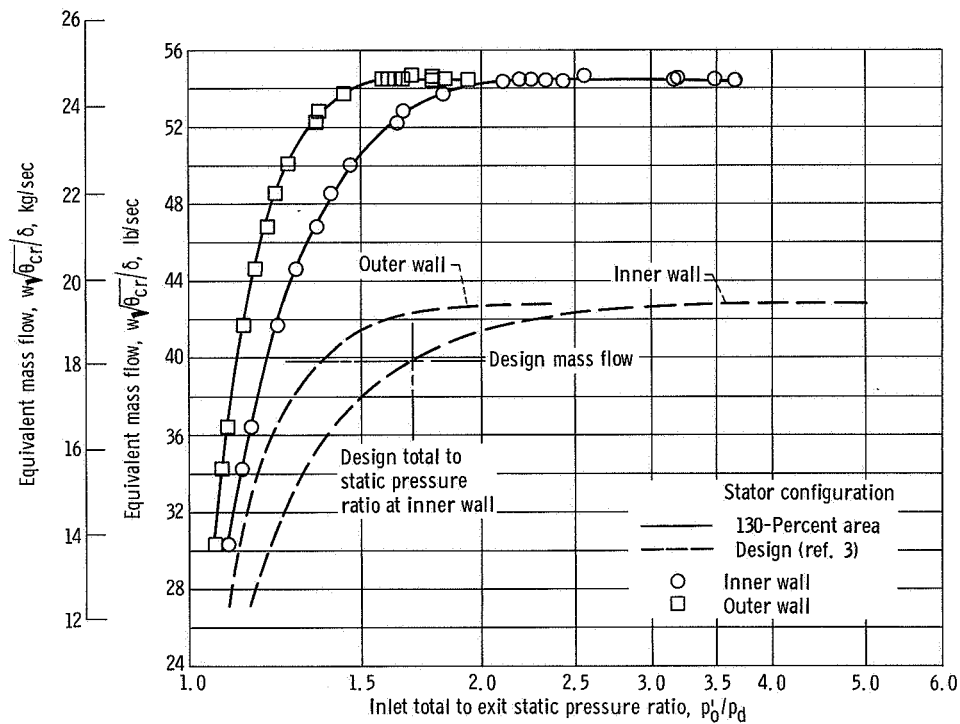
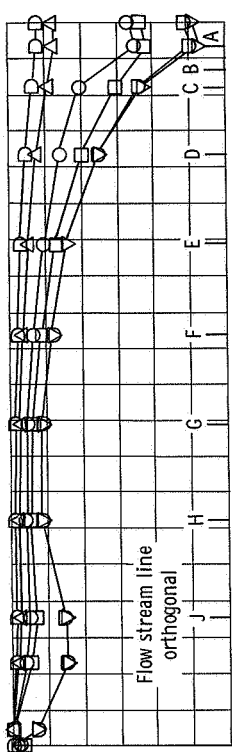Figure 6. – Variation of equivalent mass flow with total to static pressure ratio at inner and outer walls.
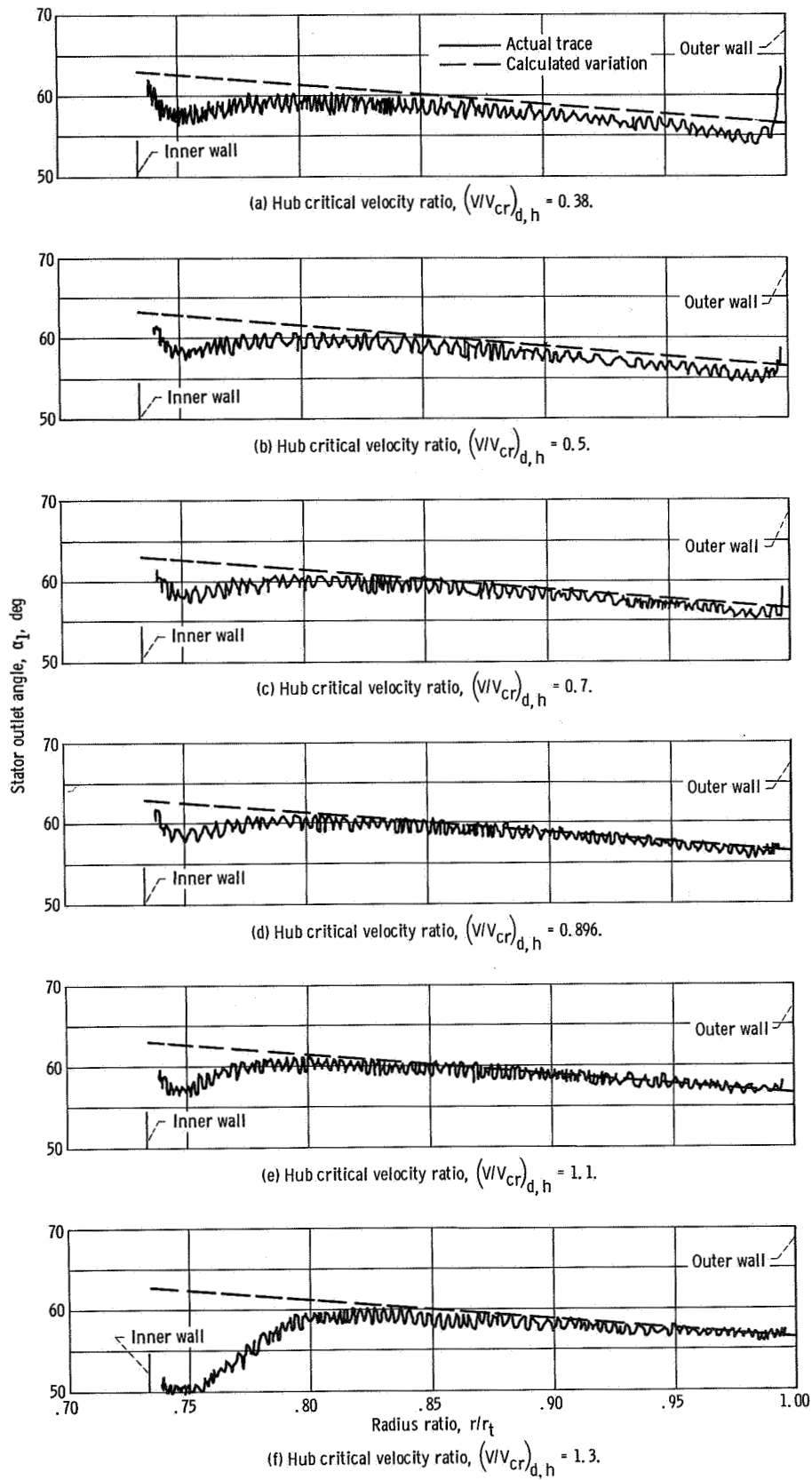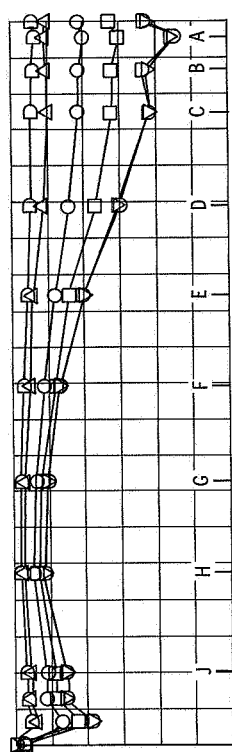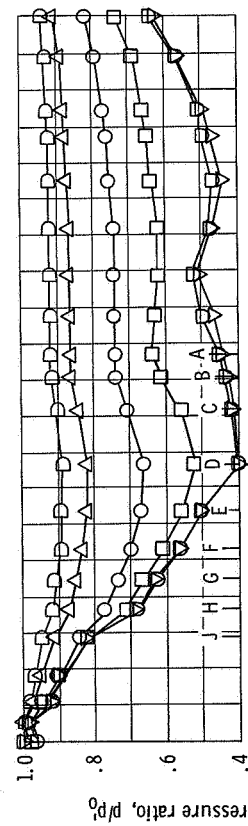
Figure 7. – Comparison of stator outlet flow angles with predicted values for a range of outlet critical velocity ratios.
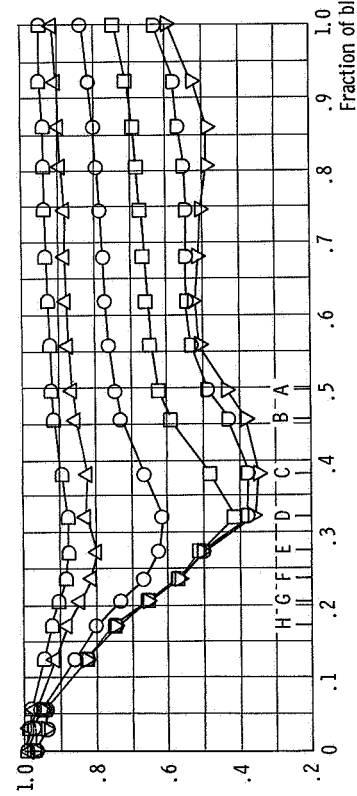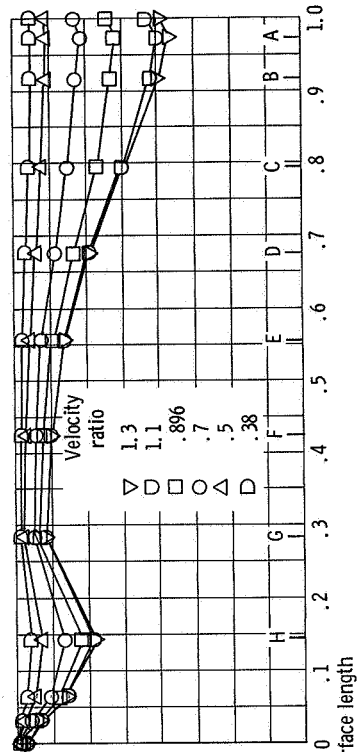
(a) Suction surface at hub section.

(b) Pressure surface at hub section.

(c) Suction surface at mean section.

(d) Pressure surface at mean section.

(e) Suction surface at tip section.

(f) Pressure surface at tip section.

Flow stream line orthogonal

Velocity ratio	
▽	1.3
◪	1.1
□	.896
○	.7
◁	.5
◩	.38

Pressure ratio, p/p₀

Fraction of blade surface length

Figure 8. – Blade surface pressure distribution.

17

(a-1) Hub section.

(b-1) Hub section.

(a-2) Mean section.

(b-2) Mean section.

Calculated by method of ref. 6
Calculated from experimental
pressure distribution
△   Suction surface
○   Pressure surface

(a-3) Tip section.

(b-3) Tip section.

(a) Subject opened stator.
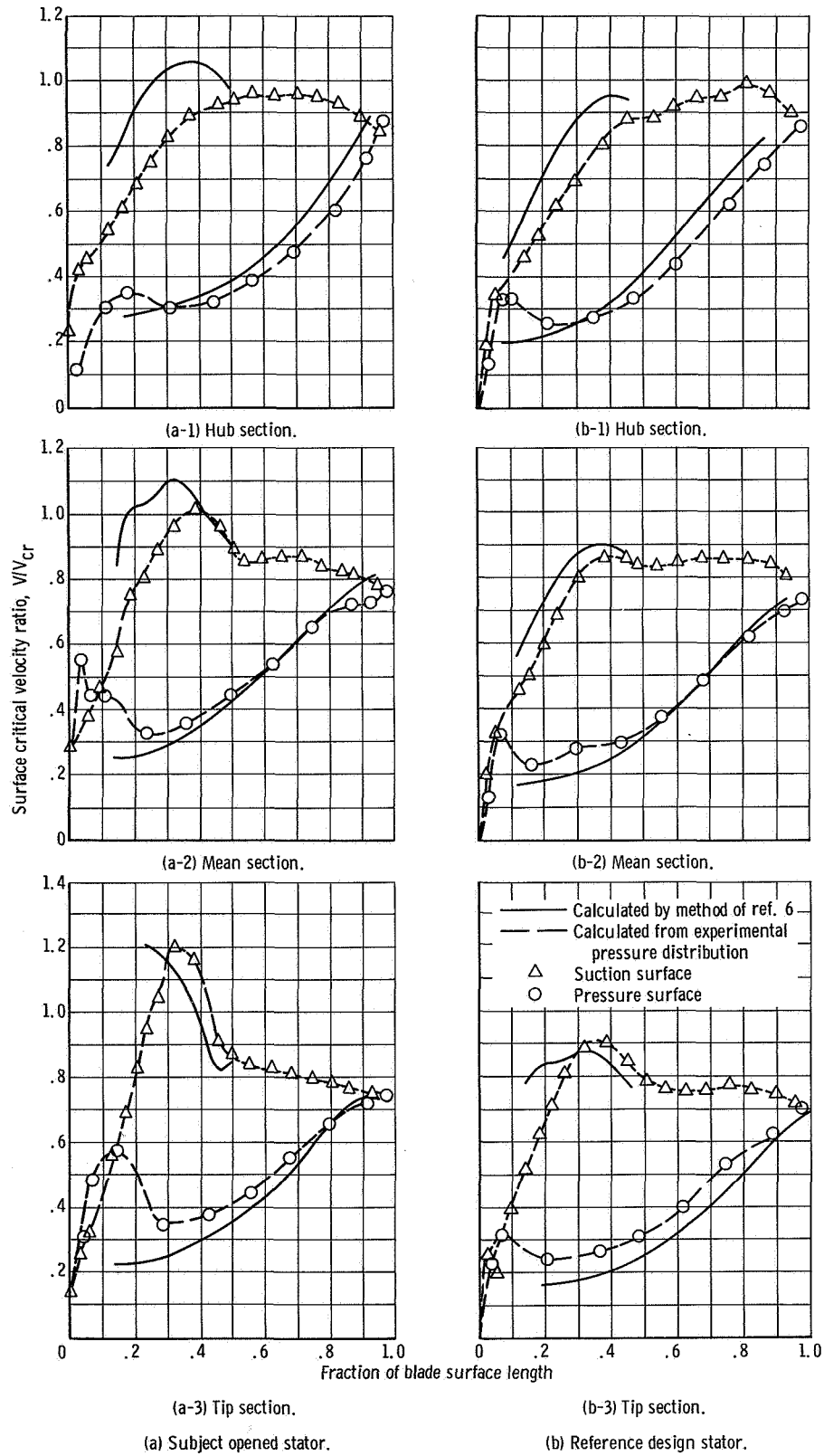
(b) Reference design stator.

Figure 9. – Comparison of calculated surface velocity with experimentally obtained surface velocity at a hub critical velocity ratio, $(V/V_{cr})_{d,h} = 0.896$.
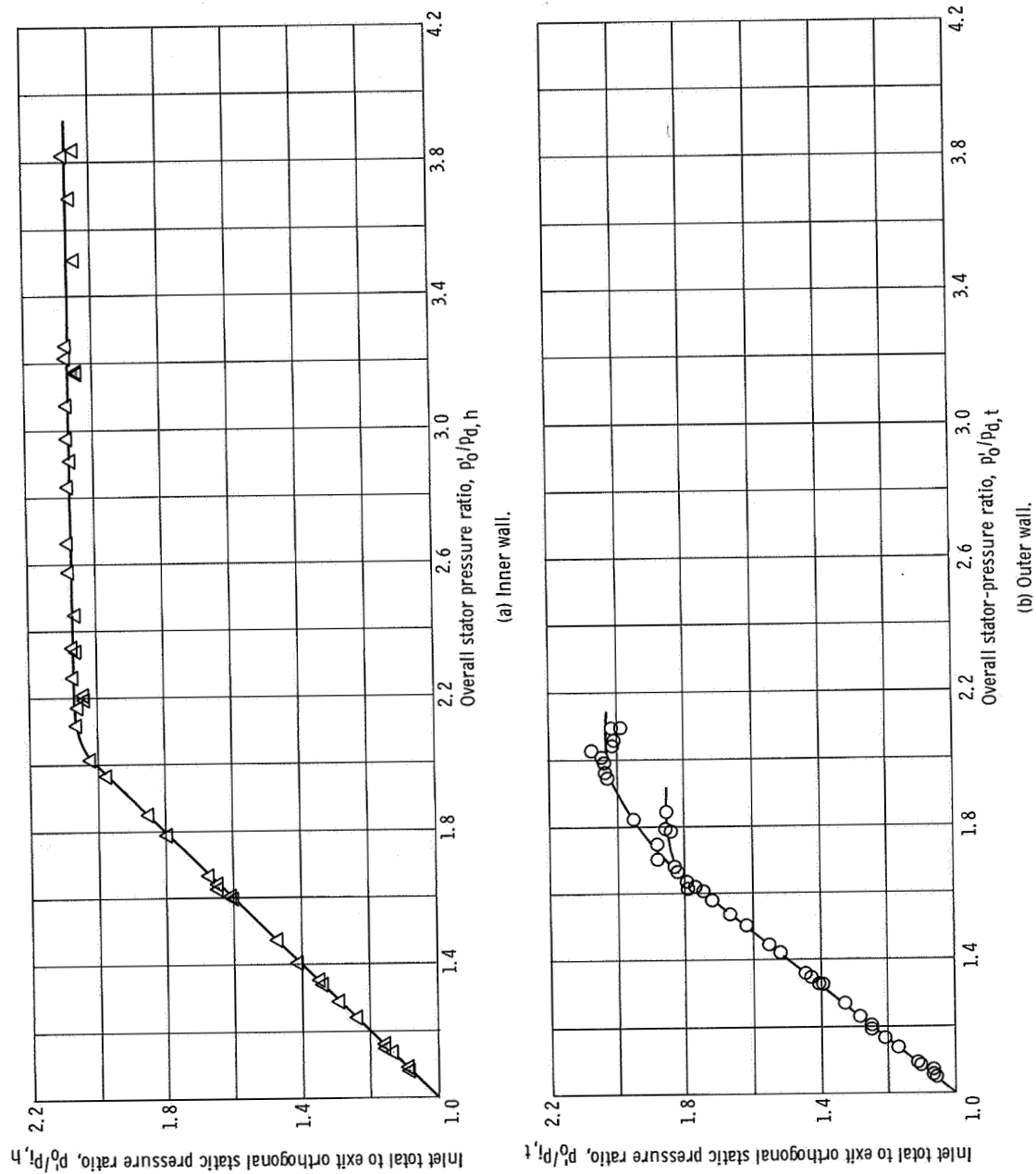
18

Figure 10. – Variation of channel exit orthogonal pressure with overall stator pressure ratio.

(a) Inner wall.

(b) Outer wall.